Journal of Power Sources 412 (2019) 677–682

Contents lists available at ScienceDirect

Journal of Power Sources

journal homepage: www.elsevier.com/locate/jpowsour

In-situ and selectively laser reduced graphene oxide sheets as excellent conductive additive for high rate capability $LiFePO_4$ lithium ion batteries

Jun Tang[a,b], Xiongwei Zhong[b], Haiqiao Li[b], Yan Li[b], Feng Pan[a,*], Baomin Xu[b,**]

[a] School of Advanced Materials, Peking University Shenzhen Graduate School, Shenzhen, Guangdong Province, 518055, China
[b] Department of Materials Science and Engineering, Southern University of Science and Technology, Shenzhen, Guangdong Province, 518055, China

HIGHLIGHTS

- An *in-situ* laser reduction of GO technique is developed without damaging $LiFePO_4$.
- *In-situ* laser rGO shows hierarchical structure for fast electron and ion transport.
- $LiFePO_4$ with *in-situ* laser rGO as conductive additive shows high rate capability.

GRAPHICAL ABSTRACT

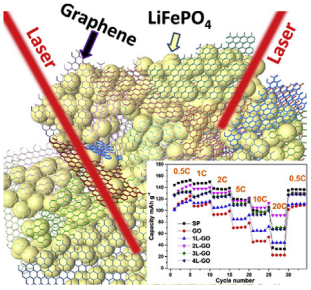

ARTICLE INFO

Keywords:
Pulse laser reduction
Graphene oxide
Ultra-fast charge/discharge
Long cycle life
Lithium ion battery

ABSTRACT

We report an ultrafast in-situ laser reduction process of graphene oxides (GO) in $LiFePO_4$ electrodes, where the selective laser reduction of GO sheets is conducted after coating $LiFePO_4$ on current collector. This novel process technique avoids the solvophobicity and agglomeration problems of graphene in 1-methyl-2-pyrrolidinone (NMP) or other solvents for the electrode material slurry preparation because of GO's solvophilicity in various solvents. Under the optimized laser reduction condition, a hierarchical structure of graphene conductive network is formed without wrapping the $LiFePO_4$ surface, which can greatly improve the rate capability and cycle performance. The battery capacity remains 84.5% after 1000 cycles and 72.9% when the charge/discharge current density increases from 0.5C to 20C. The method developed in this work is also applicable for other material systems to selectively reduce GO for performance enhancement.

1. Introduction

Lithium iron phosphate ($LiFePO_4$) has been widely used as a cathode material for the lithium ion batteries (LIBs) used in electrical vehicles because of its low cost, ultralong lifetime, and safety [1–4]. However, $LiFePO_4$ has the olivine structure which has only 1D channels for Li^+ transport, and this greatly limits its ionic conductivity. $LiFePO_4$ also shows poor electronic conductivity of only 10^{-9} S cm^{-1} [4]. To overcome the ionic and electronic transport limitations, a variety of efforts have been made, including nanosizing and carbon coating [5–13]. Nanosizing is an effective way to shorten the ionic transportation path and carbon coating to increase the conductivity of single $LiFePO_4$ particles, but the ohm contact resistance between adjacent nanosized $LiFePO_4$ particles increases because of the decreased contact area. Consequently, the $LiFePO_4$ electrode shows poor rate capability. To conquer this problem, conductive additives such as 0D acetylene

* Corresponding author.
** Corresponding author.
E-mail addresses: panfeng@pkusz.edu.cn (F. Pan), xubm@sustc.edu.cn (B. Xu).

https://doi.org/10.1016/j.jpowsour.2018.12.009
Received 30 March 2018; Received in revised form 12 November 2018; Accepted 4 December 2018
0378-7753/

black nano particles, 1D carbon nanotubes and 2D graphene sheets are always added into the $LiFePO_4$ slurry as conductive additives for electrode preparation. Acetylene black has good electronic conductivity, but it can hardly form an effective interconnected conductive network for fast charge and discharge. 1D carbon nanotubes (CNT) and 2D graphene sheets can form effective interconnected conductive networks because of their intertexture properties. However, both CNT and graphene are easily aggregated and sovlephobic, their dispersion problem in $LiFePO_4$ slurry remains to be solved, especially for industry production case where the $LiFePO_4$ slurry is highly concentrated. Reduced graphene oxide (rGO) has better solvephilic property because of its defects and residual functional groups [14]. However, when rGO is used as the starting material, the rGO sheets will wrap the $LiFePO_4$ particles and hinder the Li^+ ion transport from electrolyte to the $LiFePO_4$ surface. *In-situ* reduction of graphene oxides (GO) after coating slurry on the current collector is an alternative strategy for conductive additive because of the solvophilic characteristic and cost effectiveness of GO. Unfortunately, conventional reduction technologies such as wet chemical reduction and high-temperature H_2 reduction are not compatible with $LiFePO_4$ electrode fabrication process which is strict to the water content and intolerant to high temperatures because of organic binders. Laser reduction is a recently developed technology for fast and direct GO reduction which can yield expanded graphene with high conductivity of 1738 $S\,m^{-1}$ [15–17]. Here in this work, we are the first to apply the laser reduction technology to *in-situ* reduction of GO additive in $LiFePO_4$ electrode. Fully reduced, high-quality graphene is obtained, without damaging the $LiFePO_4$ particles and other materials in the electrode, through combining cautiously controlling the laser power density and laser scan times. The reduced graphene constructed a hierarchical structure which has the conductive network containing large graphene films covering the top of the electrode and small graphene pieces inserted into the space of $LiFePO_4$ particles. Both the large graphene film and small graphene sheet are not wrapping on the $LiFePO_4$ surface. This special hierarchical conductive network can form a high speed electronic channel without hindering the Li^+ ion transport, which improves the rate performance of $LiFePO_4$ electrode. This novel laser reduction technique developed in this work is also applicable for other material systems to selectively reduce GO, such as other anode and cathode systems for lithium ion or other batteries and supercapacitors, or other energy-storage relevant materials where graphene is needed for performance improvement.

2. Experimental section

2.1. Electrode preparation and laser reduction condition optimization

Carbon coated $LiFePO_4$ (BTR China Co., Ltd.) and Super P C45 (SP) (Shenzhen MTI. Co., Ltd.) powders were first mixed by a vortex mixer (IKA VORTEX 1). The mixture was then slowly added into PVDF-NMP solution. The final weight ratio of $LiFePO_4$, Super P and PVDF is 85:10:5. The mixture was then slowly stirred for 2 h to form $LiFePO_4$ slurry. The slurry was then slide coated onto an aluminum foil and dried at 80 °C for another 2 h and finally the $LiFePO_4$/SP electrode was obtained. The $LiFePO_4$/GO electrode was obtained by the same approach. The final slurry containing $LiFePO_4$, GO and PVDF with a weight ratio of 75:20:5.

The $LiFePO_4$/GO electrode was reduced with a pulse fiber laser. The wavelength of the laser is 1064 nm. The output laser has 100 ns pulse width and 20 kHz repetition rate. The output laser power is 3.11 Walt which is measured by a laser power meter. We adjust the laser power density through changing the distance between the focal lens and the surface of the sample, which changes the laser spot size on the sample surface. When the distance between the focal length and the surface of the sample is 7.5 cm, the laser beam is focused on the sample surface, and this gives the smallest laser spot, which is 32 μm in diameter measured by SEM (Fig. S1), and the highest laser power density, which is 387 kW/cm^2. However, this laser power density is too high, and the electrode will be totally destroyed. Hence, we reduce the laser power density by defocusing, which gives larger laser spot size, or smaller laser power density. We found that when the distance between the focal lens and the surface of the sample is 6 cm, we can selectively reduce GO without damaging the electrode. At this position, the laser spot size is 460 μm and the laser power density is 1.87 kW/cm^2 (Table S1).

While with this laser power condition we can reduce GO without damaging the electrode, the performance of the device is not optimized. We believe this is because the GO in the electrode is not totally reduced with a single laser. Hence, we use multiple scan times to get more GO reduced. As shown in the paper, 2 times scanning gives the best overall performance of the devices.

It is worth to point out that the $LiFePO_4$/GO electrode was irradiated by laser scanning with a fast line speed of 2 m/s. Therefore, even for the electrode with 3 cm × 3 cm size, it only takes 3s to finish one scan.

2.2. Battery assembly and electrochemical measurement

The final electrodes were then punched into pellets with a diameter of 12 mm. The pellets were finally assembled into 2025 coin cells together with Celgard 3501 separator and Lithium anode. 12 wt% $LiPF_6$ and 1 wt% VC were dissolved into EC-EMC-DMC (1: 1: 1 by weight) as electrolyte. The electrochemical tests were conducted using a battery test channels system (LAND-CT2001A).

2.3. Sample characterization

Scanning electron microscopy (SEM) analysis was carried out with a TESCAN SEM. X-ray diffraction (XRD) measurements were performed on a Shimadzu thin film diffractometer equipped with Copper Kα radiation (λ = 1.540598 Å) (Bruker D8 Advance ECO). The Raman Spectra were obtained using a Horiba Raman Spectrometer with 632.8 nm laser excitation.

3. Results and discussion

Scheme 1 shows the schematic illustration of *in-situ* laser reduction process. In a typically process, the electrode slurry was first prepared containing $LiFePO_4$, GO and Polyvinylidene Fluoride (PVDF). Then the slurry was coated on an aluminum substrate and dried and finally laser

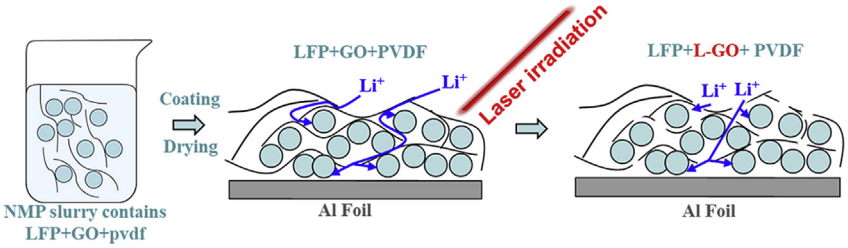

Scheme 1. Schematic illustration of in-situ laser reduction process.

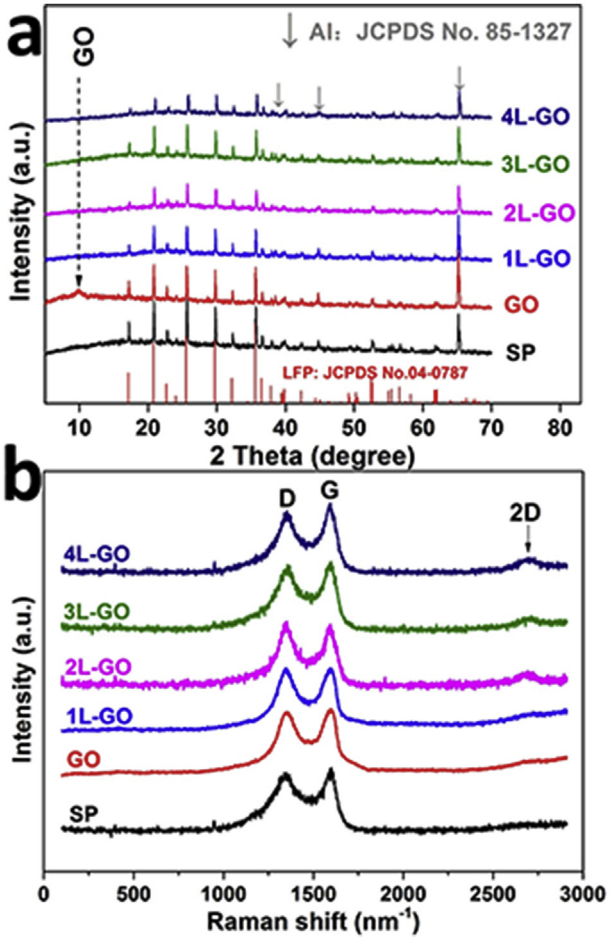

Fig. 1. (a) XRD and (b) Raman results of $LiFePO_4$ electrodes with different conductive additives.

reduced for different times. Fig. 1a shows the X-Ray Diffraction (XRD) results of $LiFePO_4$ electrodes with different conductive additives. $LiFePO_4$/Super P (SP) electrode (abbreviated as SP) shows olivine crystal structure. Diffraction peaks of $LiFePO_4$/GO electrode (denoted as GO) do not change obviously except for the existence of GO peak near 10°. The $LiFePO_4$/GO electrodes which are laser reduced for 1, 2, 3 and 4 times (denoted as 1L-GO, 2L-GO, 3L-GO and 4L-GO, respectively) show the same diffraction spectra as the unreduced ones, indicating that laser reduction did not change the crystal structure of $LiFePO_4$. The GO peak near 10° disappears for all the laser reduced electrodes, revealing that GO has been successfully reduced. The bare GO film was laser reduced as well and the XRD and XPS results are shown in Fig. S2. The results in Fig. S2 reveal that both the GO relevant peaks in XRD pattern and XPS spectrum disappear after laser reduction, indicating the fully reduction of GO. It can be seen from the Raman spectra shown in Fig. 1b that 2D peaks appear around 2700 nm^{-1} for the laser reduced electrodes, indicating that graphene was obtained by laser irradiating $LiFePO_4$/GO electrodes. Since no $LiFePO_4$ peaks were found in the Raman spectra, the laser reduction process did not damage the carbon coatings on $LiFePO_4$ surface.

Fig. 2 shows the SEM images of $LiFePO_4$ electrodes with conductive additives of SP, GO, 1L-GO, 2L-GO, 3L-GO and 4L-GO, respectively. Fig. 2a shows that Super P nano particles are not uniformly distributed among $LiFePO_4$ particles. Plenty of $LiFePO_4$ particles are isolated from the conductive highway formed by SP nano particles. Hence, poor electronic conductivity was resulted by this fragmentary conductive network when charged/discharged with high current density. It can be seen from Fig. 2b that $LiFePO_4$ particles can be fully wrapped by GO films with sufficient contact area, which means GO films will be the ideal highway for electron transportation if only GO is conductive. Unfortunately, GO is almost insulative. *In-situ* laser is an effecitive way to keep this ideal highway structure and converts the insulative GO into conductive graphene. The morphology of bare GO film will change considerably by laser reduction which is shown in Fig. S3. Interestingly, the morphology of laser reduced $LiFePO_4$/GO electrodes does not change much as shown in Fig. 2c–f, which means the conductive highway can be successfully remained.

Fig. 3a shows the schematic structure of laser reduced $LiFePO_4$/GO electrodes where larger reduced GO films work as electronic super highway and smaller fragmental reduced GO sheets work as electronic "bridges" connecting adjacent $LiFePO_4$ particles. Fig. 3b shows the corresponding SEM image of a typical hierarchical structure of the conductive network of 2L-GO electrode. The enlarged magnification of rectangular area c and area d noted in Fig. 3b are shown in Fig. 3c and d, respectively. It shows that the large continuous laser reduced GO films which work as electronic conductive highway covering the majority of the electrode surface and the fragmental reduced GO sheets which work as the conductive bridge connecting the adjacent $LiFePO_4$ particles. This unique structure ensures the effective electron transportation to every single $LiFePO_4$ particle and thus high rate capability can be expected.

Fig. 4a shows the rate capability of different $LiFePO_4$ electrodes. The corresponding charge/discharge curves are shown in Fig. S5. When charged/discharged at 0.5C, $LiFePO_4$/SP electrode shows the highest capacity. However, it drops rapidly when the charge/discharge current density increases. This result can be ascribed to the incomplete conductive network formed by Super P particles which is displayed in SEM images in Fig. 2a. $LiFePO_4$/GO electrode shows the worst performance because GO is almost insulative material and hinders the electronic and ion transport. All the laser reduced $LiFePO_4$/GO electrodes show improved capacities at high current density of 20C. The 2L-GO electrode shows the best rate performance and 73% of its initial capacity remains when the current density increases from 0.5C to 20C. The capacities of all the electrodes are restored when the current density drops back from 20C to 2C, revealing the excellent reversibility of $LiFePO_4$ electrodes. The rate performance of 2L-GO is even better than the electrode with 25% super P as conductive additive, showing a structural advantage of the graphene conductive network (Fig. S8). Fig. 4b shows the coulombic efficiency at the switch point from low current density to higher current density. The coulombic efficiency is almost the same for 2L-GO, 3L-GO, 4L-GO and SP electrodes at the current switch points of 0.5C–1C, 1C–2C and 2C–5C. However, when the current density increased from 5C to 10C, and 10C–20C, the coulombic efficiency of 2L-GO remained the highest value, which contributes greatly to the high rate performance. The high rate capability and coulombic efficiency of 2L-GO can be ascribed to the hierarchical structure of graphene conductive network induced by the *in-situ* laser reduction. The charge/discharge curves of 2L-GO electrode at 10C shows the smallest charge/discharge plateau difference, indicating the lowest inner resistance. The performance of the laser reduced $LiFePO_4$/GO electrodes strongly depends on the quality of reduction and the amount of reduced conductive products. The reduction quality means the degree of reduction thoroughness which is obviously depend on the laser power density. Higher laser power density brings higher conductivity of reduced GO. But if the laser power density is too high, the $LiFePO_4$ particles will be re-sintered and grow to larger ones, as shown in Fig. S4, which will decrease the rate capability of the electrode. Therefore, the laser power density in this work is lowered to selectively reduce GO without damaging the $LiFePO_4$ particles. However, the lowered laser power density may not be the perfect power to get the GO sheets fully reduced, which is proved by the XPS results shown in Figs. S9 and S10. This could be the reason why the performance of 1L-GO electrode is not so good as that of 2L-GO electrode. On the other hand, when bare GO film or GO in $LiFePO_4$ electrodes is reduced by laser, the reduced products

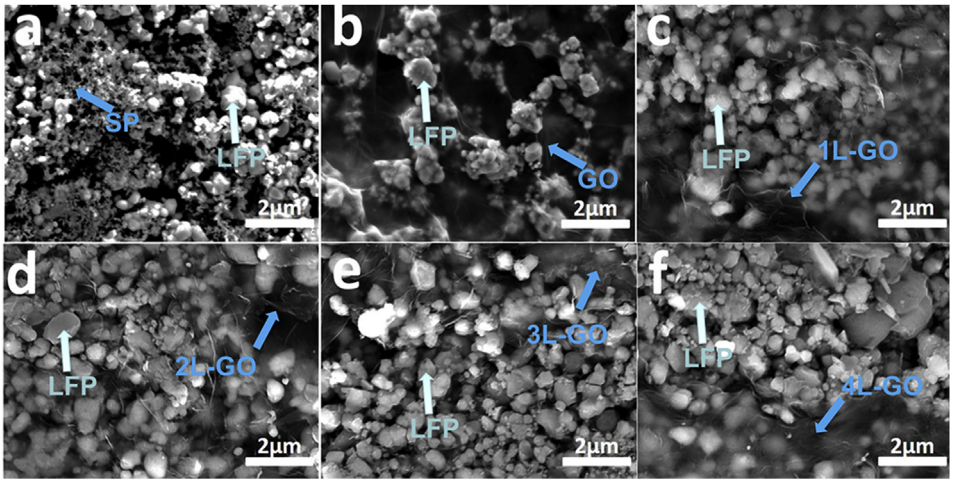

Fig. 2. SEM images of $LiFePO_4$ electrodes with different conductive additives: (a) SP, (b) GO, (c) 1L-GO, (d) 2L-GO, (e) 3L-GO and (f) 4L-GO.

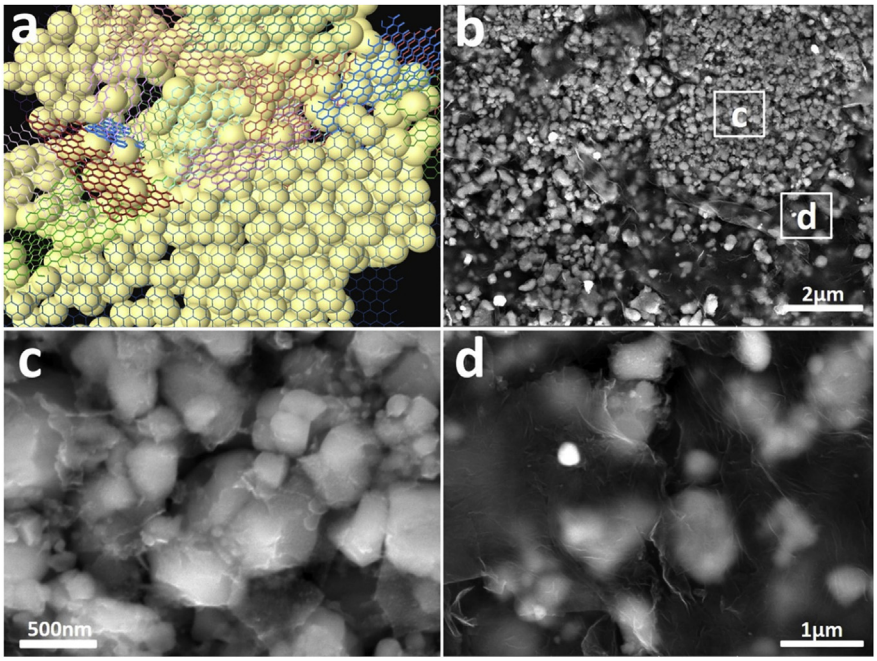

Fig. 3. (a) Schematic illustration and (b) SEM of the hierarchical structure of 2L-GO graphene conductive network, (c) smaller fragmental reduced GO sheets work as electronic "bridges" connecting adjacent $LiFePO_4$ particles, and (d) larger reduced GO films work as electronic super highway.

can be partially brought out of the electrode by the gas by-products as black smokes are observed during the reduction process. With more laser scan times, there will be more loss of the reduced products, which could decrease the rate performance of $LiFePO_4$ electrodes. This may be the reason why the performance of the 3L-GO and 4L-GO electrode is also not so good as that of 2L-GO electrode. Fig. S7 directly shows the amount difference of reduced products where graphene area (dark area) decreases obviously with laser reduction times. Table 2S also shows that there is continuous mass loss of the electrode material with more laser scan times. It is believed that 2 times' laser reduction gives an optimized balance between reduction degree and residual amount of rGO. As Fig. S10 shows, the P, C and O contents calculated from the XPS results vary significantly with the laser reduction time. The P content increases with the laser reduction time, indicating the removal of GO and XPS signal approaches more LFP particle surfaces (Fig. S10b). The increase in P content brings a rise in O content for 3L-GO and 4L-GO. The O content in 2L-GO decreases compared to 1L-GO, indicating the removal of O in the 2nd laser process overwhelms the O increase (Fig. S10c). The C content shows a highest value at 2L-GO, showing a direct reason for the high rate performance of 2L-GO (Fig. S10d). As XPS results only reflects the content relationship in a very small area and several nanometer range in depth, the C content and C/O atomic ratio variations with laser reduction times from EDS results are also showed in Fig. S11. As shown in Figure S11f, S11g, the C atomic content also shows a maximum for 2L-GO. The C/O atomic ratio also reaches the highest value when laser reduced for 2 times, indicating that 2 times' laser reduction gives an optimized balance between reduction degree and residual amount of rGO.

The 2L-GO electrode also shows the best cyclic stability when cycled at a current density of 2C, and 84.5% of its initial capacity is remained after 1000 cycles, as given in Fig. 4c. The capacity of SP electrode decreases rapidly and can only work for less than 200 times. The excellent cycling performance of 2L-GO electrode is expected but the mechanism of the cycling performance improvement remains to be further explored.

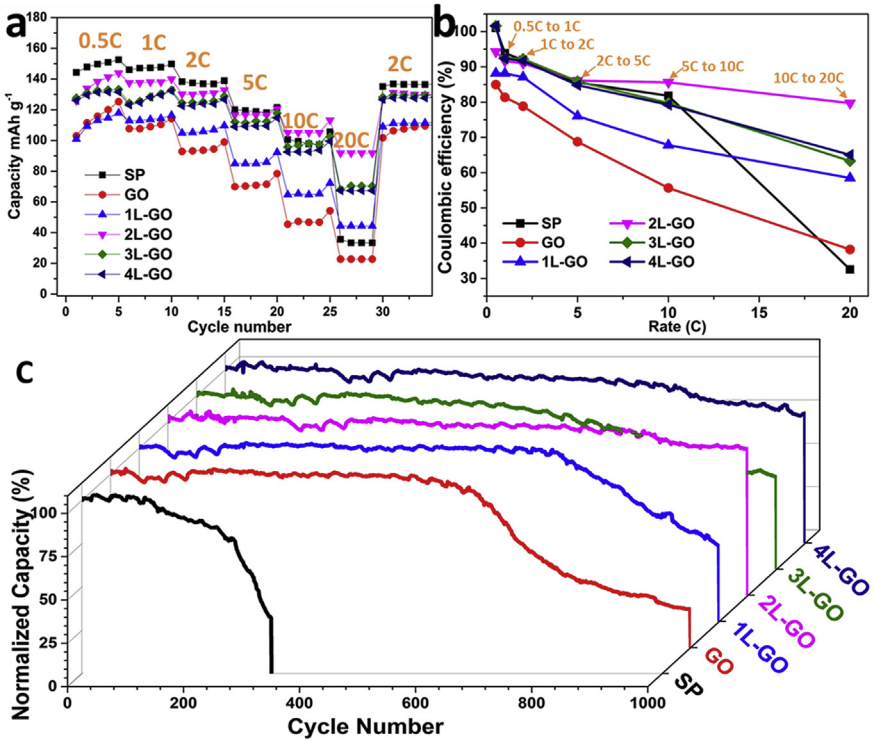

Fig. 4. (a) Rate capability curves of $LiFePO_4$ electrodes with different conductivity at different charge/discharge current densities, (b) coulombic efficiency at the switch point from low current density to higher current density, (c) cycle performance.

4. Conclusions

In-situ laser reduction is an effective approach to reduce GO in $LiFePO_4$/GO electrodes. Laser power density is the key point to selectively reduce the GO in $LiFePO_4$/GO electrodes without damaging other materials. Optimized repeated laser scan pulses is a knack for better device performance with decreased laser power density. This unique reduction process yields a hierarchical structure of graphene conductive network, which can greatly improve the rate capability and cycle performance of $LiFePO_4$ electrodes. This novel laser reduction process is fast, facile, low cost and environmental friendly, showing great application potential in battery manufacturing for high performance lithium ion batteries.

Conflicts of interest

There are no conflicts to declare.

Acknowledgements

This work is supported by the Fundamental Research (Discipline Arrangement) project funding from Shenzhen Science and Technology Innovation Committee (Grant No. JCYJ20170412154554048), the Peacock Team Project funding from Shenzhen Science and Technology Innovation Committee (Grant No. KQTD2015033110182370), the National Key Research and Development Project funding from the Ministry of Science and Technology of China (Grants Nos. 2016YFA0202400 and 2016YFA0202404), the Shenzhen Maker Project for Students (Grant No. GRCK2016041217190247), the Guangdong Innovation Team Project (No. 2013N080), and the Shenzhen Peacock Plan (Grant No. KYPT20141016105435850).

Appendix A. Supplementary data

Supplementary data to this article can be found online at https://doi.org/10.1016/j.jpowsour.2018.12.009.

References

[1] S.B. Schougaard, A nanoview of battery operation, Science 353 (2016) 543–544.
[2] B. Kang, G. Ceder, Battery materials for ultrafast charging and discharging, Nature 458 (2009) 190–193.
[3] P.-E. Delannoy, B. Riou, T. Brousse, J. Le Bideau, D. Guyomard, B. Lestriez, Ink-jet printed porous composite LiFePO4 electrode from aqueous suspension for microbatteries, J. Power Sources 287 (2015) 261–268.
[4] J. Yang, J. Wang, Y. Tang, D. Wang, X. Li, Y. Hu, R. Li, G. Liang, T.-K. Sham, X. Sun, LiFePO4–graphene as a superior cathode material for rechargeable lithium batteries: impact of stacked graphene and unfolded graphene, Energy Environ. Sci. 6 (2013) 1521.
[5] B. Wang, T. Liu, A. Liu, G. Liu, L. Wang, T. Gao, D. Wang, X.S. Zhao, A hierarchical porous C@LiFePO4/carbon nanotubes microsphere composite for high-rate lithium-ion batteries: combined experimental and theoretical study, Adv. Energy Mater. 6 (2016) 1600426.
[6] S.W. Oh, S.-T. Myung, S.-M. Oh, K.H. Oh, K. Amine, B. Scrosati, Y.-K. Sun, Double carbon coating of LiFePO4 as high rate electrode for rechargeable lithium batteries, Adv. Mater. 22 (2010) 4842–4845.
[7] A. Paolella, G. Bertoni, S. Marras, E. Dilena, M. Colombo, M. Prato, A. Riedinger, M. Povia, A. Ansaldo, K. Zaghib, L. Manna, C. George, Etched colloidal LiFePO4 nanoplatelets toward high-rate capable Li-ion battery electrodes, Nano Lett. 14 (2014) 6828–6835.
[8] Y. Duan, B. Zhang, J. Zheng, J. Hu, J. Wen, D.J. Miller, P. Yan, T. Liu, H. Guo, W. Li, X. Song, Z. Zhuo, C. Liu, H. Tang, R. Tan, Z. Chen, Y. Ren, Y. Lin, W. Yang, C.-M. Wang, L.-W. Wang, J. Lu, K. Amine, F. Pan, Excess Li-ion storage on reconstructed surfaces of nanocrystals to boost battery performance, Nano Lett. 17 (2017) 6018–6026.
[9] H. Wang, R. Wang, L. Liu, S. Jiang, L. Ni, X. Bie, X. Yang, J. Hu, Z. Wang, H. Chen, L. Zhu, D. Zhang, Y. Wei, Z. Zhang, S. Qiu, F. Pan, In-situ self-polymerization restriction to form core-shell LiFePO 4/C nanocomposite with ultrafast rate capability for high-power Li-ion batteries, Nanomater. Energy 39 (2017) 346–354.
[10] G. Arnold, J. Garche, R. Hemmer, S. Ströbele, C. Vogler, M. Wohlfahrt-Mehrens, Fine-particle lithium iron phosphate LiFePO4 synthesized by a new low-cost aqueous precipitation technique, J. Power Sources 119 (2003) 247–251.
[11] A.K. Padhi, K.S. Nanjundaswamy, J.B. Goodenough, Phospho-olivines as positive-electrode materials for rechargeable lithium batteries, J. Electrochem. Soc. 144 (1997) 1188–1194.
[12] S. Yang, P.Y. Zavalij, M. Stanley Whittingham, Hydrothermal synthesis of lithium iron phosphate cathodes, Electrochem. Commun. 3 (2001) 505–508.
[13] X.-L. Wu, L.-Y. Jiang, F.-F. Cao, Y.-G. Guo, L.-J. Wan, LiFePO4 nanoparticles embedded in a nanoporous carbon matrix: superior cathode material for electrochemical energy-storage devices, Adv. Mater. 21 (2009) 2710.

[14] E. Hu, X.-Y. Yu, F. Chen, Y. Wu, Y. Hu, X.W.D. Lou, Graphene layers-wrapped Fe/Fe$_5$C$_2$ nanoparticles supported on N-doped graphene nanosheets for highly efficient oxygen reduction, Adv. Energy Mater. 8 (2018) 1702476.
[15] M.F. El-Kady, M. Ihns, M. Li, J.Y. Hwang, M.F. Mousavi, L. Chaney, A.T. Lech, R.B. Kaner, Engineering three-dimensional hybrid supercapacitors and micro-supercapacitors for high-performance integrated energy storage, Proc. Natl. Acad. Sci. Unit. States Am. 112 (2015) 4233–4238.
[16] M.F. El-Kady, R.B. Kaner, Direct laser writing of graphene electronics, ACS Nano 8 (2014) 8725–8729.
[17] M.F. El-Kady, V. Strong, S. Dubin, R.B. Kaner, Laser scribing of high-performance and flexible graphene-based electrochemical capacitors, Science 335 (2012) 1326–1330.